Eur Biophys J (1995) 24: 13–21

European Biophysics Journal
© Springer-Verlag 1995

Study of the motion of magnetotactic bacteria

Flavio S. Nogueira[1], **Henrique G. P. Lins de Barros**[2]

[1] Centro Brasileiro de Pesquisas Físicas, R. Dr. Xavier Sigaud 150, CEP 22290-180, Rio de Janeiro, RJ-Brasil
(e-mail: FLAVIOSN@BRLNCC.BITNET)
[2] Museu de Astronomia e Ciências Afins, R. General Bruce 586, CEP 20921-030, Rio de Janeiro, RJ-Brasil (Fax: 011-21-580-4531)

Received: 14 March 1994 / Accepted in revised form: 5 October 1994

Abstract. Motion of flagellate bacteria is considered from the point of view of rigid body mechanics. As a general case we consider a flagellate coccus magnetotactic bacterium swimming in a fluid in the presence of an external magnetic field. The proposed model generalizes previous approaches to the problem and allows one to access parameters of the motion that can be measured experimentally. The results suggest that the strong helical pattern observed in typical trajectories of magnetotactic bacteria can be a biological advantage complementary to magnetic orientation. In the particular case of zero magnetic interaction the model describes the motion of a non-magnetotactic coccus bacterium swimming in a fluid. Theoretical calculations based on experimental results are compared with the experimental track obtained by dark field optical microscopy.

Key words: Bacterial motion – Magnetotaxis – Microorganism motility

1. Introduction

Motile bacteria swim by means of flagella (Berg 1975), which consist of rigid helical tubes containing a single type of protein subunit. Each flagellum is attached at its base to a protein disc embedded in the bacterial membrane by a flexible hook. This disc is part of a molecular motor (Manson et al. 1977), that produces a torque on flagellum to rotate and turns it. Several flagellar filaments emerge randomly on the sides of the bacterial body.

Two rotational directions with respect to the axis parallel to the velocity are observed. Clockwise rotation, when the angular velocity is anti-parallel to the velocity direction, and counterclockwise rotation. Counterclockwise rotation makes flagellar filaments form a synchronous bundle that pushes the bacterial body forward. On the other hand, clockwise rotation disperses flagellar filaments and each flagellum turns independently. In this last case the bacterium tumbles (Berg 1975).

It is observed that cells align the axis of their helical trajectory with the direction of the stimulus. This behavior is strikingly observed in the case of magnetotactic bacteria. Magnetotactic microorganisms are motile cells that possess intracellular magnetic particles (Blakermore 1975; Lins de Barros and Esquivel 1985; Farina et al. 1990; Mann et al. 1990; Lins de Barros et al. 1990; Lins de Barros et al. 1991) which impart to the cell a permanent magnetic dipole moment. Each intracellular magnetic particle is enveloped by a membrane forming a specialized organelle, the magnetosome (Fig. 1). The permanent cell magnetic moment interacts with an external magnetic field. This interaction produces a torque on the cell body that orients the cell to the field line. Reversion of the external field produces a new orientation of the cell and the resulting trajectory is U-shaped (Esquivel and Lins de Barros 1986).

Two types of magnetotactic microorganisms with respect to the relative magnetic dipole orientation are found in natural samples (Lins de Barros et al. 1990). South-seeking microorganisms, found preferentially in the south magnetic hemisphere, are microorganisms in which the magnetic dipole is antiparallel to the motion direction. These organisms orient to the local field line and swim downward in the south magnetic hemisphere. North-seeking microorganisms are similar to the south-seeking cells but the magnetic dipole is in the opposite direction. They swim downward in the north magnetic hemisphere. At the geomagnetic equator the geomagnetic field is parallel to the earth's surface and both magnetotactic microorganisms are found in the approximately the same proportion (Frankel et al. 1981). Magnetotaxis, that is the motility directed by a magnetic field, seems to be an adaptive mechanism in which the magnetic field acts as a stimulus (Lins de Barros et al. 1990).

In this work we study the helical motion of a coccus bacterium with a single flagellum. As a general case we consider a magnetotactic coccus bacterium swimming in a homogeneous fluid and in the presence of an external magnetic field.

Correspondence to: H. G. P. Lins de Barros

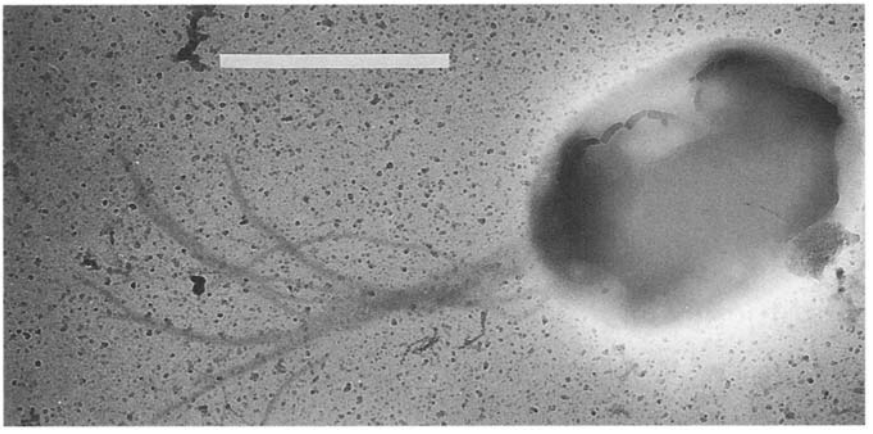

Fig. 1. Micrography of a coccus magnetotactic bacterium. It is clearly observed that the flagellar bundle emerges from only one point on the cell membrane, in contrast with *E. coli* or *Salmonella*, where the flagellar bundle emerges from several points of the cells membrane. We can observe intracellular magnetic crystals responsible for the magnetic orientation of the cell. Note that the crystal chain is nearly parallel to the flagellar axis. *Bar*=1 μm

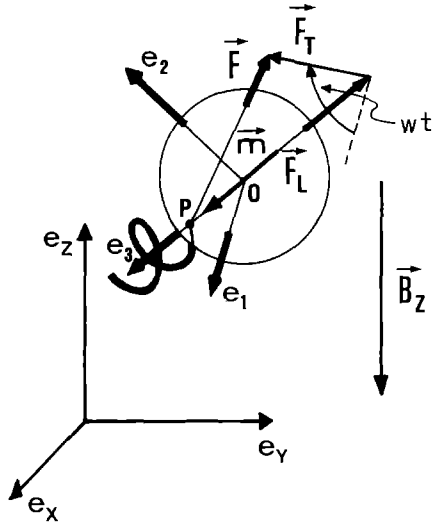

Fig. 2. Set of orthogonal axes that are used. (e_1, e_2, e_3) are unit vectors fixed respect to the cell body with origin at the center of mass. These unit vectors define the BAC reference frame. (e_1, e_2, e_3) rotates with respect to the unit vectors (e_X, e_Y, e_Z) which defines the LAB references frame. F is the propulsive force. F_3 and F_{12} are, respectively, the components of F along e_3 and in the 12-plane. F rotates with a vector angular frequency $\omega = \omega e_3$ with respect to (e_1, e_2, e_3). m is the magnetic moment of the cell which is assumed to collinear to e_3. B is the external magnetic field, assumed collinear be to e_z: For $t<0$, B is parallel to e_z while for $t<0$, B is anti-parallel to e_z. P is the point of insertion of the flagellum

Studies on the motion of magnetotactic bacteria usually specialize in U-turn analysis and application of the Bean model (Kalmijn 1981; Frankel 1984; Esquivel and Lins de Barros 1986). However, studies based on the Bean model, though the results obtained are very interesting, suffer several limitations. The main deficiency of the Bean model is that the helical pattern of the trajectory is neglected. Since experimental evidence shows that this helical pattern is very pronounced in magnetotactic organisms, it is desirable to get a model which takes this feature into account. This will be the purpose of this work. The general case considered is that of a spherical magnetotactic bacterium swimming in an iostopic viscous medium under the flagellum action.

Experimental observations were made using dark field high resolution optical microscopy with the low exposure photo technique. This procedure enables one to obtain a track of a bacterium swimming in a viscous medium. This track is interpreted as the two-dimensional projection of a tridimensional helical path on the plane of the emulsion.

2. Mathematical model

The motion of a bacterium in a viscous medium is characterized by a condition of very low Reynolds number (Purcell 1977). Reynolds number is a dimensionless parameter given by the ratio between inertial and viscous forces. In a very low Reynolds number regime no inertial effects are observed.

Let us consider a spherical magnetotactic bacterium with radius R propelled by a force F (due to flagellar action) that acts at a fixed point P (the point of insertion of the flagellar bundle) on the cellular membrane. The cell possesses a permanent magnetic moment, m. The bacterium swims in a fluid with viscosity η. This propulsive force, F, is not generally collinear with the flagellar axis (Schreiner 1971). If the flagellum rotates around its axis with angular frequency ω relative to the cell body, F is written as

$$F = F_{12}(\cos\omega\, te_1 + \sin\omega\, te_2) + F_3 e_3 \qquad (2.1)$$

where the first term simulates the action of a flagellum with a non-integer number of turns. F_{12} and F_3 are constants. (e_1, e_2, e_3) are unit vectors defining a reference frame fixed with respect to the cell body with origin at the center of mass O of the cell. We denote this reference frame by BAC. This set of unit vectors rotates in a general way relative to the set of unit vectors (e_x, e_y, e_z) defining an auxiliary reference frame CM with origin in O that translates with respect to an inertial reference frame fixed in the laboratory (LAB). The LAB frame is specified by the unit vectors (e_X, e_Y, e_Z). With no loss of generality we take CM as being parallel to LAB, that is, $e_x // e_X$, $e_y // e_Y$, $e_z // e_Z$. We treat the motion of the bacterium with the usual formalism of rigid body dynamics: First we describe the rotation of BAC with respect to CM and then we describe

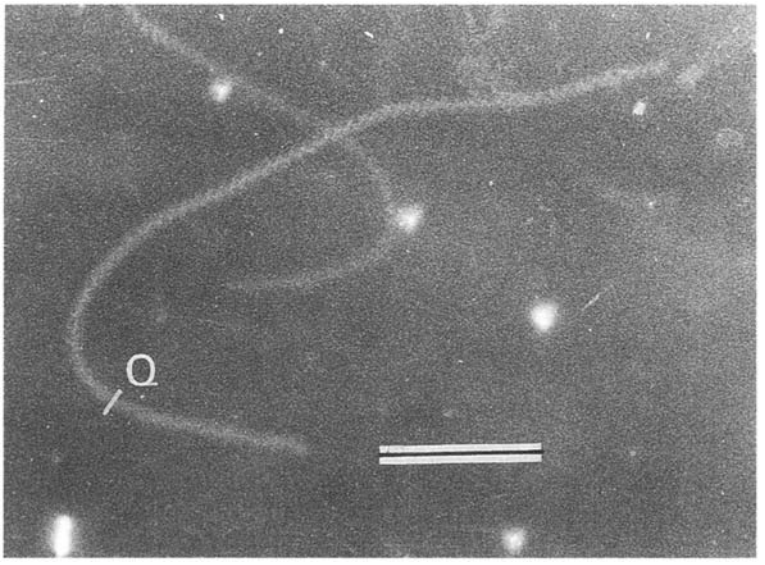

Fig. 3. Experimental track of a magnetotactic bacterium obtained by the low exposure dark field optical micrography technique. The external applied magnetic field was suddenly reversed when the bacterium was at **Q**. The samples were observed with a coverslip to ensure good focus condition. This procedure allows us to obtain a record of a trajectory nearly confined to a plane. *Bar*=30 μm. Time of exposure = 1.6 s

translation of CM with respect to LAB. In LAB, the coordinates of the common origin of BAC and CM are given by the components of the vector $\boldsymbol{r}=x\,\boldsymbol{e}_X+y\,\boldsymbol{e}_Y+z\,\boldsymbol{e}_Z$. In the BAC reference frame the point of insertion P is given by the vector $R\boldsymbol{e}_3$ (Fig. 2).

As the bacterium swims under the action of the propulsive force given by (2.1) it suffers the action of a hydrodynamic force $\boldsymbol{F}_H$. Evaluation of this force at low Reynolds number requires the solution of an unsteady Navier-Stokes equation since (2.1) is time-dependent. However, we can simplify considerably the analysis if we note that the characteristic time scale for this problem is typically of $O(R^2/\nu)=O(10^{-6})$ (ν is the kinematic viscosity). The force $\boldsymbol{F}$ oscillates with period $T=2\pi\omega^{-1}=O(10^{-1})$ *sec* which is a typical value for magnetotactic bacteria. Since in this case $T\gg R^2/\nu$ one has a pseudo-steady regime (Lamb 1932, p 642–644) and we take the hydrodynamic force acting on the spherical bacterium as having only viscous components. Thus, we approximate the hydrodynamic force as a pseudo-steady stokes drag:[1]

$$\boldsymbol{F}_H(t)=-6\pi\eta R\,\boldsymbol{v}(t) \tag{2.2}$$

where $\boldsymbol{v}(t)$ is the velocity vector and $\boldsymbol{F}_H$ acts on O. Note that in contrast to the steady Stokes drag, we have in (2.2) a time-dependent velocity vector.

On the basis of the approximation made in (2.2), we assume that there is a balance between $\boldsymbol{F}$ and $\boldsymbol{F}_H$, that is, at each instant of time the usual Stokes law holds and that inertia is irrelevant. In the case $F_{12}=0$, which corresponds to a flagellum with an integer number of turns (Schreiner 1971; Berg 1983, p 78–79) we have $\boldsymbol{F}=F_3\boldsymbol{e}_3$ and we can treat the problem as a true steady state regime. However, since the motion of magnetotactic bacteria usually exhibits a strong helical pattern (Fig. 3), F_{12} gives in a very significant contribution. Therefore in this work $F_{12}\neq 0$ and situations in which $F_{12}=0$ are treated as particular cases. Therefore, according to Newtons second law, disregarding inertial contributions[2],

$$\boldsymbol{F}+\boldsymbol{F}_H=O \tag{2.3}$$

Solving for $\boldsymbol{v}$:

$$\boldsymbol{v}=v_{12}(\cos\omega t\boldsymbol{e}_1+\sin\omega t\boldsymbol{e}_2)+v_3\boldsymbol{e}_3 \tag{2.4}$$

where

$$v_{12}=\frac{F_{12}}{6\pi\eta R} \tag{2.5}$$

$$v_3=\frac{F_3}{6\pi\eta R} \tag{2.6}$$

Note that the velocity vector is not colinear with the flagellar axis, $\boldsymbol{e}_3$, but precesses around it.

Before further work with (2.4) in order to obtain the differential equations for translation of center of mass, let us consider first the rotational equations of motion.

In the approximation considered, the rotational equations of motion with respect to BAC, are given in vector form as:

$$\boldsymbol{N}_C+\boldsymbol{N}+\boldsymbol{N}_H+\boldsymbol{N}_m=O. \tag{2.7}$$

In the above, $\boldsymbol{N}_C$ denotes the reaction couple due to the couple that generates flagellar rotation with frequency ω. $\boldsymbol{N}_C$ is constant since ω is constant. It is given by

$$\boldsymbol{N}_C=-N_C\boldsymbol{e}_3 \tag{2.8}$$

with $N_C>0$.

$\boldsymbol{N}$ is the torque produced by $\boldsymbol{F}$ given by

$$\boldsymbol{N}=\boldsymbol{R}\times\boldsymbol{F}=N_{12}(-\sin\omega t\boldsymbol{e}_1+\cos\omega t\boldsymbol{e}_2) \tag{2.9}$$

with $N_{12}=RF_{12}$. $\boldsymbol{R}$ is given by $\boldsymbol{R}=R\boldsymbol{e}_3$.

[1] For a recent discussion on arbitrary time-dependent motions at small Reynolds number see, for example, Lovalenti and Brady (1993)

[2] We have neglected a pure inertial contribution in the hydrodynamic force (the so called added mass) which is of the same order as the inertia in Newton's is second law

N_H is the hydrodynamic torque. For the same reasons as before, we consider here a pseudo-steady rotation drag. For a spherical body rotating in a viscous medium one has (Lamb 1932; p 642)

$$N_H(t)=8\pi\eta R^3\,\boldsymbol{\Omega}(t) \tag{2.10}$$

where $\boldsymbol{\Omega}$ is the angular velocity vector of the cell body whose components are written in terms of Euler angles as (Goldstein 1980; p 176)

$$\Omega_1=\dot{\phi}\sin\theta\sin\psi+\dot{\theta}\cos\psi \tag{2.11}$$
$$\Omega_2=\dot{\phi}\sin\theta\cos\psi-\dot{\theta}\sin\psi \tag{2.12}$$
$$\Omega_3=\dot{\phi}\cos\theta+\dot{\psi} \tag{2.13}$$

where the dots denote total time differentiation. Finally, N_m is the magnetic torque. To evaluate this torque it is necessary to assume an applied magnetic field, $\boldsymbol{B}$. There is no loss of generality to assume $\boldsymbol{B}$ collinear to $\boldsymbol{e}_z$. We consider B constant. At $t>0$ $\boldsymbol{B}$ is anti-parallel to $\boldsymbol{e}_z$. Assuming, for simplicity, the magnetic moment, $\boldsymbol{m}$, collinear to $\boldsymbol{e}_3$ we write

$$\boldsymbol{m}=m\boldsymbol{e}_3 \tag{2.14}$$

$$\boldsymbol{B}=\begin{cases} B\boldsymbol{e}_z \text{ if } t<0 \\ -B\boldsymbol{e}_z \text{ if } t>0 \end{cases} \tag{2.15}$$

with B=const. This gives for $t>0$ the magnetic torque

$$\boldsymbol{N}_m=\boldsymbol{m}\times\boldsymbol{B}=mB\sin\theta\,\boldsymbol{e}_N \tag{2.16}$$

where $\boldsymbol{e}_N$ is a unit vector directed along the line of nodes:

$$\boldsymbol{e}_N=\cos\psi\,\boldsymbol{e}_1-\sin\psi\,\boldsymbol{e}_2 \tag{2.17}$$

The Euler equations of motion for the bacterium, for $t>0$, are

$$\Omega_1=-\alpha\sin\omega t+\beta\sin\theta\cos\psi \tag{2.18}$$
$$\Omega_2=\alpha\cos\omega t-\beta\sin\theta\sin\psi \tag{2.19}$$
$$\Omega_3=-\gamma \tag{2.20}$$

where

$$\alpha=\frac{N_{12}}{8\pi\eta R^3} \tag{2.21}$$

$$\beta=\frac{mB}{8\pi\eta R^3} \tag{2.22}$$

$$\gamma=\frac{N_C}{8\pi\eta R^3} \tag{2.23}$$

Substituting (2.11–13) into (2.18–20) and solving for the angular velocities $\dot{\phi}$, $\dot{\theta}$ and $\dot{\psi}$, one obtains

$$\dot{\phi}=\alpha\,csc\,\theta\cos(\omega t+\psi) \tag{2.24}$$
$$\dot{\theta}=\beta\sin\theta-\alpha\sin(\omega t+\psi) \tag{2.25}$$
$$\dot{\psi}=-\gamma-\alpha\cot\theta\cos(\omega t+\psi). \tag{2.26}$$

The above equations describe the rotation of the cell body with respect to CM.

In order to obtain the equations of motion for the translation of the center of mass we should transform the equation obtained for $\boldsymbol{v}$, Eq. (2.4), which is written in terms of the unit vectors $(\boldsymbol{e}_1, \boldsymbol{e}_2, \boldsymbol{e}_3)$, to the unit vectors $(\boldsymbol{e}_X, \boldsymbol{e}_Y, \boldsymbol{e}_Z)$. Taking into account that in this reference frame the components of $\boldsymbol{v}$ are $(\dot{x}, \dot{y}, \dot{z})$, one obtains after some algebra involving the transformation matrix relating the two frames (Goldstein 1980; p 147), the following equations of motion for the center of mass:

$$\dot{x}=v_{12}\left[\cos\phi\cos(\omega t+\psi)-\sin\phi\cos\theta\sin(\omega t+\psi)\right]+v_3\sin\phi\sin\theta \tag{2.27}$$

$$\dot{y}=v_{12}\left[\sin\phi\cos(\omega t+\psi)+\cos\phi\cos\theta\sin(\omega t+\psi)\right]-v_3\sin\theta\cos\phi \tag{2.28}$$

$$\dot{z}=v_{12}\sin\theta\sin(\omega t+\psi)+v_3\cos\theta \tag{2.29}$$

Note that the magnitude of $\boldsymbol{v}$ is $v=(v_{12}^2+v_3^2)^{1/2}$=const. Using (2.5) and (2.21) we have

$$v_{12}=\frac{4}{3}\alpha R \tag{2.30}$$

Equations (2.24–26) together with (2.27–29) completely determine the motion of a magnetotactic bacterium with six degrees of freedom.

An important formula that will be useful in the subsequent analysis relates $\dot{\boldsymbol{v}}$ to $\boldsymbol{v}$. Let us take the time derivative of $\boldsymbol{v}$:

$$\dot{\boldsymbol{v}}=\boldsymbol{\omega}\times\boldsymbol{v}+v_{12}(\cos\omega t\,\dot{\boldsymbol{e}}_1+\sin\omega t\,\dot{\boldsymbol{e}}_2)+v_3\,\dot{\boldsymbol{e}}_3 \tag{2.31}$$

with $\boldsymbol{\omega}=\omega\boldsymbol{e}_3$. Using the vector relations for orthogonal unit vectors, we evaluate the time derivative of the unit vectors above to obtain $\boldsymbol{v}$ with respect to LAB.

$$\dot{\boldsymbol{v}}=(\boldsymbol{\omega}+\boldsymbol{\Omega})\times\boldsymbol{v} \tag{2.32}$$

Equation (2.32) shows that the angular velocity of the vector $\boldsymbol{v}$ is given by $\boldsymbol{\Gamma}=\boldsymbol{\omega}+\boldsymbol{\Omega}$. Since $\boldsymbol{v}$ is tangent to the trajectory, it follows that the period of the helical trajectory is $T=2\pi/\Gamma$, with

$$\Gamma=[(\omega-\gamma)^2+\alpha^2-2\alpha\beta\sin\theta\cos(\omega t+\psi)]^{1/2} \tag{2.33}$$

Note that although we are considering an approximately stationary regime, $\dot{\boldsymbol{v}}$ is not approximately zero.

3. Limit cases

(i) $\alpha=\beta=0$

This case corresponds to a non-magnetotactic bacterium with a flagellum with an integer number of turns. The equations of motion are exactly soluble and give a straight line trajectory. Explicitly, if the initial conditions are $\theta(0)=0$, $\phi(0)=0$ and $\psi(0)=0$, one has

$$\begin{aligned} \phi(t)&=0 \\ \theta(t)&=0 \\ \psi(t)&=-\gamma t \\ x(t)&=0 \\ y(t)&=0 \\ z(t)&=vt. \end{aligned} \tag{3.1}$$

In this case the cell swims with constant velocity v and rotates around its axis with constant angular velocity $-\gamma$.

(ii) $\alpha=0$

This case corresponds to a magnetotactic bacterium with a flagellum with an integer number of turns. The equations of motion reduce to the set of equations:

$$\dot{\phi} = 0 \tag{3.2}$$
$$\dot{\theta} = \beta \sin\theta \tag{3.3}$$
$$\dot{\psi} = -\gamma \tag{3.4}$$
$$\dot{x} = v_3 \sin\phi \sin\theta \tag{3.5}$$
$$\dot{y} = -v_3 \sin\theta \cos\phi \tag{3.6}$$
$$\dot{z} = v_3 \cos\theta. \tag{3.7}$$

The above equations can be integrated analytically and the resulting trajectory lies in a plane. This limit case corresponds to the Bean model (Esquivel and Lins de Barros 1986). This simplified model predicts the mean amount of time, t_u, required for a magnetotactic bacterium to reorient its magnetic moment to the magnetic field when the field is suddenly reversed and the mean diameter of the resulting U-turn, L. The U-turn time and the U-turn diameter are given, respectively, by (Esquivel and Lins de Barros 1986)

$$t_u = \frac{8\pi\eta R^3}{mB} \ln\left(\frac{2mB}{kT}\right) \tag{3.8}$$

$$L = \frac{8\pi^2 \eta R^3}{mB} v_3 \tag{3.9}$$

where k is the Boltzmann constant and T is the absolute temperature.

The solution $\theta(t)$ of (3.3) is given by

$$\theta(t) = 2\arctan\left(e^{\beta t} \tan\frac{\theta_0}{2}\right) \tag{3.10}$$

We observe that $\theta(t) \to \pi$ as $t \to \infty$.

(iii) $\alpha << \omega - \gamma$ and $\beta = 0$

This case corresponds to a non-magnetotactic bacterium whose flagellum has an almost integer number of turns. In this case an approximate analytical solution can be obtained by perturbation theory (Arnold 1973, p 64–66). The result is a solution which is an expansion in the parameter $\alpha/(\omega-\gamma)$. For a small value of the parameter, the solutions can be approximated linearly in the parameter. The result for the rotational part of motion is

$$\begin{aligned}
\phi(t) &= \frac{\alpha \csc\theta_0}{\omega-\gamma} \sin[(\omega-\gamma)t] + O(\alpha^2/(\omega-\gamma)^2) \\
\theta(t) &= \theta_0 + \frac{\alpha}{\omega-\gamma}\{\cos[(\omega-\gamma)t] - 1\} \\
&\quad + O(\alpha^2/(\omega-\gamma)^2) \\
\psi(t) &= -\gamma t - \frac{\alpha}{\omega-\gamma} \cot\theta_0 \sin[(\omega-\gamma)t] \\
&\quad + O(\alpha^2/(\omega-\gamma)^2)
\end{aligned} \tag{3.11}$$

with initial conditions $\phi(0) = \psi(0) = 0$ and $\theta(0) = \theta_0$.

The solutions $(x(t), y(t), z(t))$ are obtained by substitution of the above result in (2.27–29), expanding the right hand side of these equations keeping only terms of order $\alpha/(\omega-\gamma)$ and integrating the result. The resulting expressions are lengthy and not too illuminating, so we will omit them.

(iv) $\alpha << \omega - \gamma$ and $\beta \neq 0$

This case corresponds to a magnetotactic bacterium whose flagellum has a quasi-integer number of turns. The approximate solution up to first order in $\alpha/(\omega-\gamma)$ is

$$\begin{aligned}
\theta(t) &= \theta_{CB}(t) + \frac{\alpha}{\omega-\gamma}\{\cos[(\omega-\gamma)t] - 1\} \\
&\quad + O(\alpha^2/(\omega-\gamma)^2)
\end{aligned} \tag{3.12}$$

where $\theta_{CB}(t)$ is the solution given by (3.10). Since for $t \gg t_u$ $\theta_{CB}(t) \to \pi$, one has

$$\begin{aligned}
\theta(t >> t_u) &= \pi + \frac{\alpha}{\omega-\gamma}\{\cos[(\omega-\gamma)t] - 1\} \\
&\quad + O(\alpha^2/(\omega-\gamma)^2)
\end{aligned} \tag{3.13}$$

Equation (3.13) shows that for $t \gg t_u$, θ oscillates around $\pi - \alpha/(\omega-\gamma)$ with frequency $\omega-\gamma$ and amplitude $\alpha/(\omega-\gamma)$.

4. Applications

Samples of magnetotactic bacteria were collected in the interface water-sediment in a brackish coastal water lagoon. The samples were maintained for two weeks in a laboratory without any chemical enrichment. For optical microscopy observation a drop of water with sediment was placed on the microscope. A coverslip was used to ensure good focus conditions and to limit the movement approximately to a plane. A pair of Helmholtz coils adapted to the microscope provide a homogeneous and stable magnetic field. Residual fields, such as the geomagnetic field or induced fields on the microscope, were not compensated. Dark field illumination was used to obtain the bacterium track in the film emulsion (Esquivel and Lins de Barros 1986).

Experimental tracks obtained by the low exposure dark field optical micrography technique give the projection of the bacterium trajectory on the film emulsion plane (Fig. 3).

Electron scanning or transmission microscopy together with optical microscopy allows one to estimate the bacterium radius R. U-turn analysis allows one to estimate the cell magnetic moment[3]. The water viscosity, η, has a value of 0.01 *Poise*. The migration velocity is defined as the projection of v along the axis of the helical trajectory. It is measured directly by photography or using recorded video images (Esquivel and Lins de Barros 1986; Lins de Barros and Esquivel 1985). Experimental estimation of v_{12} or v_3 is difficult. Figure 3 shows that the portion of the trajectory far from the U-turn region can be interpreted as the projection of a helix on the emulsion plane. For this reason we assume that, in this portion of the trajectory, $\boldsymbol{v}\cdot\boldsymbol{e}_z \simeq v_3 \boldsymbol{e}_3$. This corresponds to the assumption that $\boldsymbol{e}_3$ is approximately parallel to $\boldsymbol{e}_z$ in the region of best alignment with the magnetic field (remember that the magnetic mo-

[3] For a detailed description and application of the method see, for example, Esquivel and Lins de Barros (1986)

ment is collinear with e_3). In the Bean model the alignment of e_3 with e_z occurs exactly; see (3.10). Within this assumption v_3 is interpreted as the migration velocity, which can be measured. v_{12} is obtained by measuring the mean pitch angle θ_P of the helical trajectory. Then,

$$\frac{v_{12}}{v_3} = \tan\theta_P \tag{4.1}$$

θ_P can be estimated by analysing the track obtained by dark field optical microscopy (Fig. 4). The parameter α is obtained directly from (2.30) and we obtain using (4.1)

$$\alpha = \frac{3 v_{12} \tan\theta_p}{4 R} \tag{4.2}$$

The number of cycles/sec of the helical trajectory is $\Gamma/2\pi$. Using (2.33) one has

$$\omega - \gamma = (\Gamma^2 - \alpha^2)^{1/2} \tag{4.3}$$

where the time dependent part of (2.33) is disregarded. In fact, the measurement of Γ can be made in portions of the trajectory posterior to the U-turn or in zero field regimes. For the magnitudes of the fields currently used in the laboratory the time dependent part of (2.33) does not contribute too much.

The parameters ω and γ cannot be obtained separately. However, any value can be attributed to ω and γ if one maintains the difference $\omega-\gamma$ fixed with $\gamma<\omega$.

The equations of motion were integrated numerically in a computer using a fourth order Runge-Kutta method. The estimated experimental values for the parameters used in the numerical integration are:

$R = 1.2\pm0.1$ μm
$m=(2.2\pm0.2)\times10^{-12}$ emu
$B = 2.5\pm0.1$ G
$\alpha=133\pm12$ rad/s
$\omega-\gamma=175\pm17$ rad/s
$v_3=125\pm12$ μm/s.

The intital conditions used in numerical integration are $\phi(0)=\psi(0)=0$, $x(0)=y(0)=z(0)=0$ and $\theta(0)=\left(\frac{2kT}{mB}\right)$

The value of the initial condition $\theta(0)$ is chosen by taking into account thermal disturbances (the same value of $\theta(0)$ is used in the Bean model; see Esquivel and Lins de Barros (1986)). Figure 5 shows the projection of the tridimensional computer generated trajectory in three orthogonal planes with the above parameters. Note that, in this particular case, the axis of the trajectory is nearly contained in the yz-plane. Comparison with the experimental track (Fig. 3) can be made directly because experimental procedures limit the movement in such a way that it is nearly contained in a plane. Figure 3 shows that, in the specific laboratory conditions that the photographic plate was obtained, the track is not well aligned to the external applied field (z-direction) in contrast with the obtained computer trajectory where this alignment is almost perfect (by "alignment" of the trajectory we mean alignment of the axis of the helical trajectory). This is due to a constant residual field (induced on the microscope and/or the geomagnetic field). Figure 6 shows a computer generated tra-

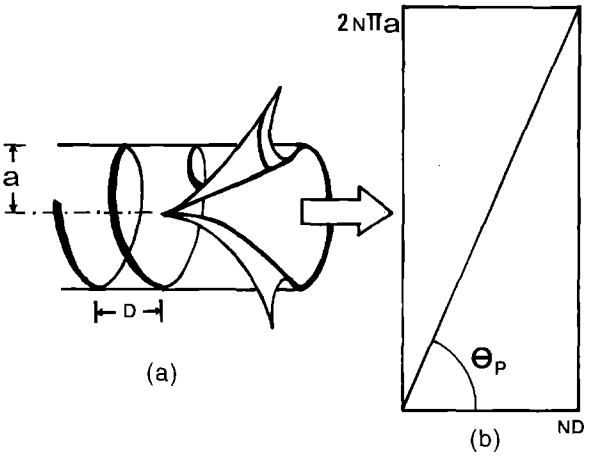

Fig. 4. Geometric determination of θ_P assuming helical trajectory. a is the helix radius, D is the pitch. N is the number of pitches considered. θ_P is the pitch angle of the helix. The helix trajectory (**a**) is cutdown to form a retangle (**b**)

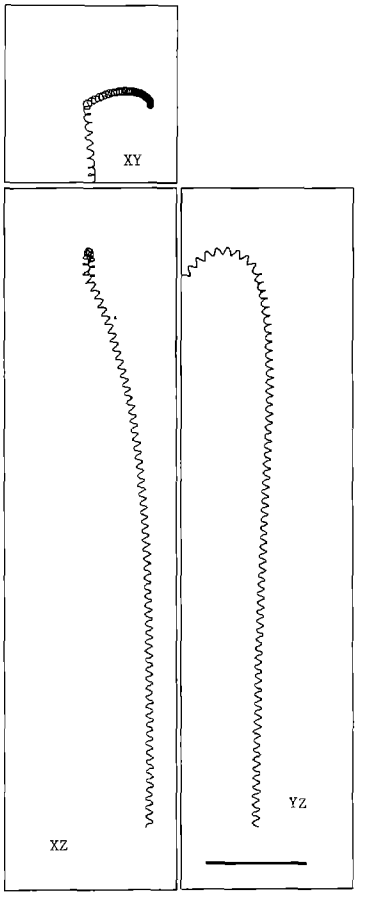

Fig. 5. Computer generated trajectory of a magnetotactic bacterium with cell radius equal to 1.2 μm, magnetic moment of 2.2×10^{-12} emu, longitudinal velocity of 125 μm/s and the frequency parameters $\alpha=133$ rad/s, $\omega-\gamma=175$ rad/s in the presence of an external constant magnetic field of 2.5 G aligned to z-direction. At $t=0$ (point **Q**) the field is suddenly reversed in order to generate a U-turn trajectory. Initial conditions are $\theta(t=0)=1.2$ rad, $\phi(t=0)=0$ and $\psi(t=0)=0$. $Bar=30$ μm

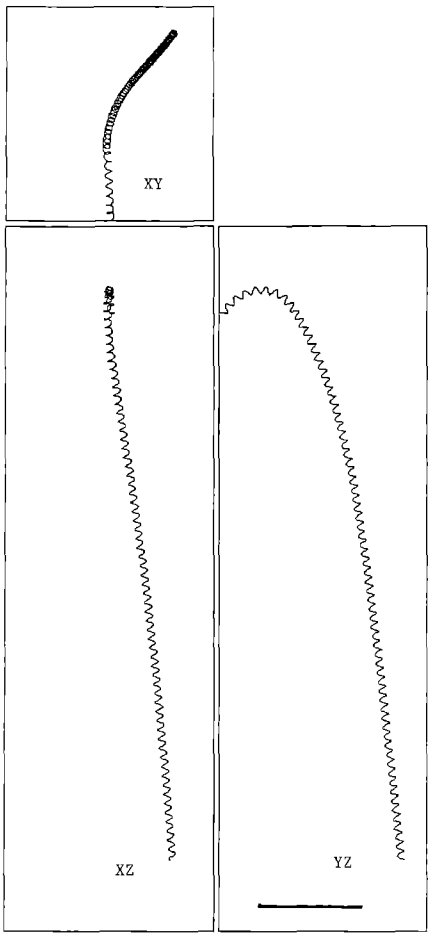

Fig. 6. Computer generated trajectory of a magnetotactic bacterium in the presence of an applied external field plus a residual field. The parameters used are identical to that of Fig. 5 except that, in addition to the field applied in z-direction there is also a residual field of 0.1 G in the y-direction. $Bar = 30\ \mu m$

jectory where a residual constant field of 0.1 G, parallel to the y-axis, was considered. Figure 7 shows a superposition of the yz-plane of the computer trajectory of Fig. 6 with the photographic plate shown in Fig. 3. The time of exposure in Fig. 3 is 1.6 while the time of motion in Fig. 6 is 2 seconds.

Figure 8 shows a computer generated trajectory of a magnetotactic bacterium (same parameters as above, except for B) in the local geomagnetic field (in Rio de Janeiro the local field is about 0.25 G). This case simulates the actual situation of a magnetotactic bacterium in its natural habitat. This computer trajectory has the same total time of motion as that in Figs. 5 and 6 (which is 2 s) and we note that there is no U-turn in this case. It is an interesting question if this bacterium performs a U-turn in the geomagnetic field after a longer time. We integrated the equations of motion up to a time of 15 s and no U-turn was observed. In this case we note a competition between magnetic and helical motion orientation mechanisms.

Finally, Fig. 9 shows a computer generated trajectory of a magnetotactic bacterium (same parameters as above, except for B) in a zero field condition ($B=0$). This case simulates the trajectory of a non-magnetotactic bacterium swimming in water.

5. Conclusions

We have described a simple model to treat the movement of a magnetotactic flagellate coccus bacterium. In the particular case of zero magnetic interaction ($B=0$ or $m=0$) this model describes the movement of a non-magnetotactic flagellate coccus bacterium swimming in a fluid. The present approach ignores all inertial contributions of the fluid or the cell body. This allows one to describe the mo-

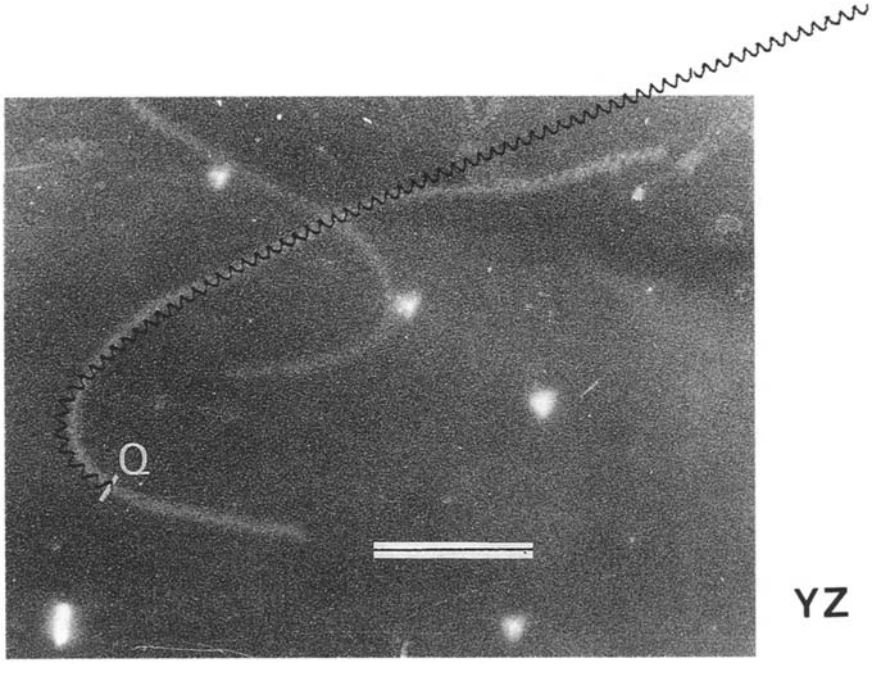

Fig. 7. Superposition of the yz-plane of the computer trajectory of Fig. 6 with the photograph showed in Fig. 3. $Bar = 30\ \mu m$

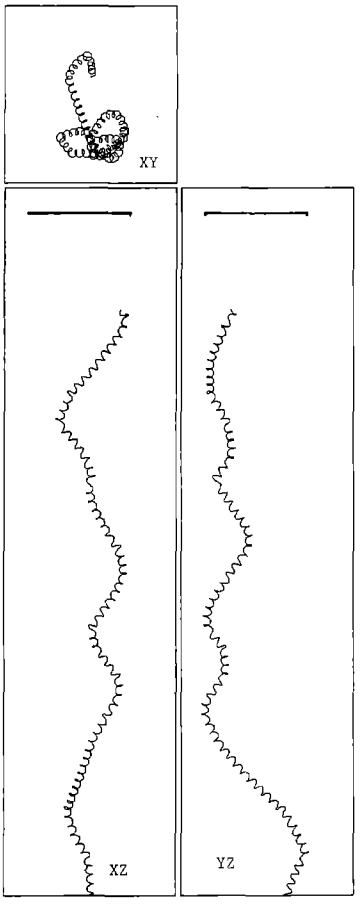

Fig. 8. Computer generated trajectory of a magnetotactic bacterium in the presence of the local geomagnetic field (0.25 G in Rio de Janeiro). All the remaining parameters are the same as for Figs. 5 and 6. $Bar=30$

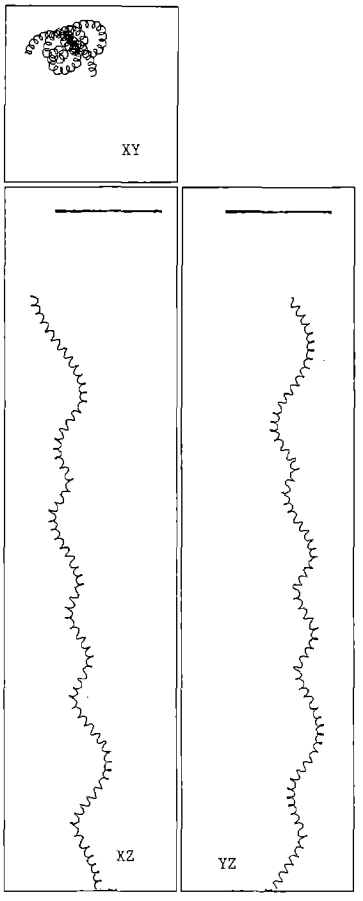

Fig. 9. Computer generated trajectory of a magnetotactic bacterium in zero field regimen. The remaining parameters are the same as for Figs. 5, 6 and 7. $Bar=30$ μm

tion with all the six degrees of freedom in a simple way. The formalism can be generalized to other cell geometries or magnetic fields.

The model proposed assumes a flagellate bacterium with only one flagellum. This is not a drastic simplification because experimental evidence shows that flagellate bacteria swim forward and make all flagella rotate counterclockwise in a cooperative way, forming a flagellar bundle. This flagellar bundle behaves as a single effective flagellum. Several magnetotactic bacteria have only one flagellar bundle. Figure 1 is an example.

With the theory developed in this work it is possible to associate all relevant theoretical parameters with the observed ones. Equation (4.3), in particular, is of fundamental importance in relating the observed trajectory to the parameter $\omega - \gamma$.

The observed matching of the theoretical trajectory (Figs. 5 and 6) with the experimental tracks is not fortuitous. We had made a calculation in several different magnetotactic bacteria and obtained approximately the same good results. The behavior of the numerical solutions shows that results are sensitive to variation of parameters. However, the change in trajectory with respect to the variation of parameters is not dramatic. Figures 5 and 6 are the best match to the experimental trajectory.

Figure 8 suggests that this bacterium does not perform a U-turn in the geomagnetic field. This is a very peculiar situation since it is widely believed that magnetotaxis is an orientation mechanism which makes the bacterium swim downward to find sedimented regions. On the basis of the theoretical and numerical results we have shown that, under the experimental conditions considered, the flagellar action dominates the magnetic interaction.

Change in flagellar frequency can occur in a natural habitat, allowing an efficient magnetic orientation. Crenshaw (1993a, b; Crenshaw and Edelstein-Keshet 1993) shows that the change in the cell body frequency, when induced by a concentration gradient, is an efficient mechanism of orientation because it changes the motion direction. This mechanism can be used by the magnetotactic bacterium to reorient to the geomagnetic field. However, as the flagellar action dominates magnetic interaction, a perfect alignment of the cell magnetic moment to the field line is far from being achieved. This does not imply that the geomagnetic field is irrelevant for the bacterium considered. In fact, the geomagnetic field here plays an important role: It acts as a bound to the helical motion, that is, the geomagnetic field avoids the upward swimming of the magnetotactic bacterium but does not constrain the motion strongly to the field line (as would be the case for a

magnetotactic bacterium whose flagellum possess an integer number of turns). This mechanism allows the bacterium to swim in a wider region. Therefore we can suggest that the helical motion performed by the magnetotactic bacterium is a biological advantage that complements the advantage of the magnetic orientation. This argument can be strongly supported if it is related to experimental observation of helical flagella in typical magnetotactic bacteria. Observed flagella of magnetotactic bacteria are very short compared to the cell body dimensions and generally do not have an integer number of turns (Fig. 1) giving a large value of the parameter α. Calculations with the same parameters used in the preceding section, except for B which is taken as the local geomagnetic field, and the small value of α shows that the bacterium makes a U-turn. Very short flagella with a non-integer number of turns, as observed in magnetotactic bacteria, can be a result of efficient adaptive factors. If the local field is sufficient to constrain strongly the movement, the magnetic orientation reduces the possibilities of motion direction. The average motion is nearly constrained to one direction, allowing a faster migration velocity. However, a bacterium strongly constrained to the magnetic field interacts very poorly with the environment and this is not biologically advantageous. If a magnetotactic bacterium has a long flagellum with an integer or quasi-integer number of turns, the geomagnetic field is sufficient to limit the bacterium to the field line.

It is possible, however, that experimental conditions used to observe magnetic response (high magnetic fields, samples in the microscope, different molecular oxygen pressure, etc.) change the state of flagellar rotation, and that, in the natural habitat, the same bacterium swims differently and may be strongly constrained to the field line. Even being aware of this possibility, we believe on the basis of the available evidence, that this is not the case. We hope that these questions can be better answered by further experimental investigation on the behavior of magnetotactic bacteria in arbitrarily small magnetic fields.

Finally, the present theory can guide experimentalists in the search of relevant parameters not directly accessible in the laboratory.

Acknowledgements. The authors would like to thank Drs. D. M. S. Esquivel (CBPF) and M. Farina (Instituto de Biofisica, UFRJ) for helpful discussion and for electron microscopy work and the Conselho Nacional de Desenvolvimento Cientifico e Tecnologico (CNPq) and Fundação de Auxílio a Pesquisa do Estado do Rio de Janeiro (FAPERJ) for financial support.

References

Arnold VI (1973) Ordinary Differential Equations. MIT Press, Cambridge

Berg HC (1975) Bacterial behaviour. Nature 254:389–392

Berg HC (1983) Random Walk in Biology. Princeton University Press, Princeton, NJ

Blakemore RP (1975) Magnetotactic bacteria. Science 190:377

Crenshaw HC (1993a) Orientation by helical motion – I. Kinematics of the helical motion of organisms with up to six degrees of freedom. Bull Math Biol 55:(1)197–212

Crenshaw HC (1993b) Orientation by the helical motion – III: Microorganisms can orient to stimuli by changing the direction of their rotational velocity. Bull Math Biol 55:(1)231–255

Crenshaw HC, Edelstein-Keshet L (1993) Orientation by helical motion – II. Changing the direction of the axis of motion. Bull Math Biol 55:(1)213–230

Esquivel DMS, Lins de Barros HGP (1986) Motion of magnetotactic microorganisms. J Exp Biol 121:153–163

Farina M, Esquivel DMS, Lins de Barros HGP (1990) Magnetic iron-sulphur crystals from magnetotactic microorganism. Nature 343:256–258

Frankel RB (1984) Magnetic guidance of organisms. Annu Rev Biophys Bioeng 13:85–103

Frankel RB, Blakemore RP, Torres de Araujo FF, Esquivel DMS, Danon J (1981) Magnetotactic bacteria at geomagnetic equator. Science 212:1269–1270

Goldstein H (1980) Classical Mechanics, 2nd edn. Addison-Wesley, Reading, Mass

Kalmijn AJ (1981) Biophysics of geomagnetic field detection. IEEE Trans. Mag 17:(1)1113–1124

Lamb H (1932) Hydrodynamics. Dover, New York

Lins de Barros HGP, Esquivel DMS (1985) Magnetotactic microorganisms found in muds from Rio de Janeiro. A general view. In: Biomineralization and Magnetoreception in Organisms. Kirschvink JL, Jones DS, Macfadden BJ (eds) Plenum Press, New York

Lins de Barros HGP, Esquivel DMS, Farina M (1990) Magnetotaxis. Sci Prog Oxford 74:347–359

Lins de Barros HGP, Esquivel DMS, Farina M (1991) Biomineralization of a new material by a magnetotactic microorganism. In: Iron Biominerals. Frankel RB, Blakemore RP (eds) Plenum Press, New York

Lovalenti PM, Brady JF (1993) The hydrodynamic force on a rigid particle undergoing arbitrary time-dependent motion at small Reynolds number. J Fluid Mech 265:561–605

Mann S, Sparks NHC, Frankel RB, Bazylinski DA, Janasch HW (1990) Biomineralization of ferrimagnetic greigite (Fe_3S_4) and iron pyrite (FeS_2) in a magnetotactic bacterium. Nature 343:258–261

Manson MD, Tedesco P, Berg HC, Harold FM, van der Drift C (1977) A protonmotive force drives bacterial flagella. Proc Natl Acad Sci, USA 74:(7)3060–3064

Purcell EM (1977) Life at low Reynolds number. Am J Phys 45:(1)3–11

Schreiner KE (1971) The helix as propeller of microorganisms. J Biomech 4:73–83